Ecotoxicology and Environmental Safety 239 (2022) 113682

Contents lists available at ScienceDirect

Ecotoxicology and Environmental Safety

journal homepage: www.elsevier.com/locate/ecoenv

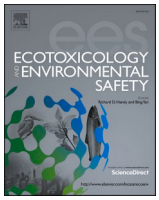

Gestational exposure to fluoride impairs cognition in C57 BL/6 J male offspring mice *via* the p-Creb1-BDNF-TrkB signaling pathway

Weisheng Li [1], Likui Lu [1], Dan Zhu, Jingliu Liu, Yajun Shi, Hongtao Zeng, Xi Yu, Jun Guo, Bin Wei, Yongle Cai, Miao Sun [*]

Institute for Fetology, The First Affiliated Hospital of Soochow University, Suzhou 215006, Jiangsu, China

A R T I C L E I N F O

Edited by Dr Yong Liang

Keywords:
Gestational exposure
Fluoride
P-Creb1-BDNF-TrkB signaling
Cognitive impairment

A B S T R A C T

Fluoride exposure has a detrimental effect on neurodevelopment, while the underlying processes remain unknown. The goal of this study was to investigate how fluoride impacts synaptogenesis, with a focus on the phosphorylation of Creb1 (p-Creb1)-brain-derived neurotrophic factor (BDNF)-tyrosine kinase B (TrkB) pathway. We generated a sodium fluoride (NaF) model using C57 BL/6 J mice exposed to 100 mg/L NaF from gestation day 1 (GD1) to GD20. It was identified that NaF treatment impaired the learning and memory abilities of the male offspring, reduced dendritic spine density, lowered postsynaptic density protein-95 (PSD95) and synaptophysin (SYN) expression in the male offspring's hippocampus, indicating that synaptic dysfunction may contribute to the cognitive impairment in the NaF model. In addition, *in vivo* experiment demonstrated that the protein abundance of BDNF and the ratio of p-Creb1 to Creb1 were increased in the hippocampus of NaF offspring, while the level of TrkB was reduced. Similarly, PC12 cells treated with NaF also showed increased expression of BDNF and decreased levels of TrkB. Notably, fluoride treatment increased p-Creb1 *in vitro*, while inhibiting p-Creb1 by 66615 significantly alleviated the effects of NaF exposure, indicating that p-Creb1 exerts a regulatory function in the BDNF-TrkB pathway. Altogether, these results demonstrated prenatal fluoride exposure triggered neurotoxicity in the male offspring hippocampus was linked to synaptogenesis damage caused by activating p-Creb1, which disrupted the BDNF-TrkB pathway.

1. Introduction

Fluoride is a chemically active element that is abundant in nature. Although certain fluoride levels can be utilized to prevent dental cavities and osteoporosis, long-term fluoride consumption might have negative consequences, such as endemic fluorosis, which mainly includes dental fluorosis and skeletal fluorosis (Darchen et al., 2016). It is assessed that more than two hundred million people globally drink water with fluoride levels higher than the recommended limitation of 1.5 mg/L by the World Health Organization (WHO) (Rasool et al., 2018). Excess fluoride may pass through the blood-brain barrier and build up in the cerebrum, posing a risk of neurological damage (Blaylock, 2004). According to epidemiologic studies, high fluoride levels in drinking water have been linked to deleterious impacts on children's neurodevelopment, including intelligence, memory and cognitive performance issues (Guth et al., 2020). Furthermore, animal research has shown that chronic fluoride exposure results in anxiety-depressive symptoms, difficulties with memory, cognition, attention, sensory-motor gating and autism spectrum disorder (Flace et al., 2010; Strunecka and Strunecky, 2019; Adkins and Brunst, 2021). Even though fluoride has long been suspected of being a developmental neurotoxin, the mechanisms behind fluoride's adverse effects on the developing brain are unknown. Hundreds of billions of synapses connect individual neurons in the brain to construct precise neural circuits that allow for optimum performance and cognitive ability (Wu et al., 2020). During infancy, inadequate synaptic formation or function results in developmental neurological diseases such as cognitive difficulties and mental retardation (Lepeta et al., 2016). Excessive fluoride exposure during perinatal has been shown to reduce PSD thickness, increase the synaptic cleft width and decrease the abundance of PSD95 and SYN in the rat hippocampus (Chen et al., 2018). However, the effects of prenatal fluoride exposure on the establishment and development of synapses and dendritic spines and the

* Corresponding author.
E-mail address: miaosunsuda@163.com (M. Sun).
[1] These authors have contributed equally to this work

https://doi.org/10.1016/j.ecoenv.2022.113682
Received 21 February 2022; Received in revised form 15 May 2022; Accepted 20 May 2022
Available online 25 May 2022

underlying mechanisms are unclear.

BDNF has been recognized as an essential regulator of cognitive performance. Neuronal survival, differentiation, dendritic growth and synaptic maturation depend on the interaction of BDNF with its specific receptor, TrkB (Miranda et al., 2019). During synaptic development and maturation, the BDNF-TrkB pathway and its intracellular signaling pathway targets, including PSD95 and SYN, are necessary for synaptic formation and maintenance (Yoshii and Constantine-Paton, 2010). Anomalies in the BDNF-TrkB pathway have been connected to the development of cognitive deficit disorders and therapeutic effects (Qiu et al., 2020). However, it is unknown whether BDNF-TrkB signaling contributes to fluoride-induced synaptic impairments. Epidemiological findings revealed that fluoride acts as a potential neurotoxin matter in utero and increased levels of fluoride exposure during pregnancy are associated with lower Intelligence Quotient (IQ) in children, especially in boys (Green et al., 2019). We employed a mouse model of prenatal fluoride exposure and cell culture assays to investigate the influence of maternal fluoride on spinogenesis and synaptogenesis in neurodevelopment, with a particular emphasis on the involvement of the BDNF-TrkB pathway and its upstream regulation in fluoride-induced neurotoxicity.

2. Materials and methods

2.1. Compounds and reagents

The sodium fluoride (#7681–49–4, St. Louis, Mo, USA) was purchased from Sigma-Aldrich, and 66615 (CREB1 inhibitor, #HY-101120, Monmouth Junction, NJ, USA) was purchased from Med Chem Express. Unless otherwise stated in the different methods, all extra components were analytical grade and bought locally.

2.2. Experimental animals

At Soochow University's experimental animal facility, mice were maintained in a pathogen-free environment. All mice were kept in cages with no more than five mice per cage with a 12-hour light/dark cycle (8 a.m. to 8 p.m.). Behavioral testing was done with a background illumination of 120 lux throughout the light process. Following the National Institutes of Health's Guidelines for the Care and Use of Laboratory Animals (NIH), the Institutional Animal Care and Use Committee at Soochow University authorized all procedures and techniques used in this study. Animals were randomly divided into two groups of ten mice: a control group and a NaF-treated group (100 mg/L). Fluoride ion concentrations have ranged from 0.01 to 48 mg/L in India (Chakrabarty, 2012). Furthermore, mice are better at expelling fluoride from their systems than humans, and those consuming water containing 100 mg/L NaF exhibited blood fluoride levels comparable to individuals taking water containing 5–10 mg/L fluoride ion (DenBesten, 2011; Lyaruu, 2008). Based on the population's ambient exposure levels, the biological features of mice and past research on mice, our current study employed fluoride concentrations of 100 mg/L NaF (Cao, 2016; Fu, 2022; Wang, 2021). Male and female mice (1:1) were randomly mated overnight in each group. Pregnant mice were maintained separately in cages with identical environmental and exposure settings until pups were weaned. A part of the fetus at embryonic day 20 was collected and excised for the experiment. Behavioral studies were scheduled for the male offspring from the sixth to eighth week after birth. After intraperitoneal injection of sodium pentobarbital, the transverse chamber of the mice was opened to expose the chest cavity and the right atrial appendage was gently cut open with scissors before being perfused with 50 ml PBS solution three times through the left ventricle. Finally, the mice were killed by exsanguination through the abdominal aorta. After immediately decapitating the mice, the skull was cut open along the sagittal suture, the brain tissues were carefully removed, the cerebellum was separated along the midline and then the white matter was gently peeled off with a curved forceps and the hippocampal tissue was removed. Parts of hippocampus tissues were formalin-fixed and paraffin wax-embedded for HE and Nissl staining, while other parts were promptly frozen in liquid nitrogen and preserved at − 80 °C for future research.

2.3. Behavior tests

2.3.1. Morris Water Maze (MWM) test

The cognitive capacities of mice were assessed in MWM for five days in a row. A black-painted circular water tank (120 cm in diameter, 50 cm in height), an unseen black platform (round, 6 cm in diameter), and a video camera positioned above the middle of the water tank and linked to a tracking system (ANY-maze, Japan) in an adjacent room were combined to build up the MWM. At a temperature of 22 ± 2 °C, the tank was filled to a depth of 30 cm with water (adding nontoxic white paint). At the northeast quadrant's center, the platform was hidden 1 cm below the liquid level (seen as the target quadrant). The memory training lasted four days. The maximum time it could take to find the platform was one minute, or until it climbed up. The mice that couldn't find the platform in one minute were led there. Mice were allowed 15 s on the platform before being towel dried and placed in a waiting cage for 15 min to allow them to rebuild physical capacity before moving on to the next session. Mice were put in the pool at varying starting points for four trials on each training day. The hidden platform was removed on the fifth day, and a single trial was undertaken to test memory. Each mouse was given one minute to swim freely.

2.3.2. Rotarod test

The rotarod apparatus (Zhenghua, Anhui, China) was used to assess coordination ability. On two consecutive days, the mice were trained for three times five minutes trials at 5 rpm, and the test was conducted on the third day. The revolving rod was accelerated from 0 to 40 rpm in five minutes during the test. The average time stayed on the rod for three trials was used to determine the latency to fall off the rotarod.

2.3.3. Open field test

The open field test apparatus (40 ×40 ×40 cm^3) comprises opaque white plastic barriers. The mice were placed in the center of the open field test apparatus. Their motions in the open field test apparatus were captured throughout a six minutes session. As previously indicated, both center entries and time spent in the central region (20 ×20 cm^2) were recorded by a tracking system (ANY-maze, Japan) (Li et al., 2016).

2.3.4. Elevated plus maze test

The elevated plus maze apparatus was around 70 cm above ground level. The labyrinth comprises two opposed open arms (30 cm × 5 cm) and two opposing closed arms with opaque walls 14 cm high. At the start of the experiment, the mice were put in the center of the elevated plus maze, facing open arms, and their movements were monitored for ten minutes by a tracking system (ANY-maze, Japan). After each test, the maze was washed with a 75% ethanol solution to remove mouse odor. As previously indicated, time spent in closed and open arms was separately recorded (Kraeuter et al., 2019).

2.3.5. Tail suspension test

Mice tails were attached to the shelf's edge and hung 35 cm above the surface. A tracking system (ANY-maze, Japan) was used to record the immobility time, which did not include the time spent struggling.

2.3.6. Forced swim test

Each mouse was placed in a cylindrical glass container with a diameter of 15 cm and a height of 20 cm, which was filled with water (23–25 °C) to a depth of 14 cm. The length of immobility was defined as the period during which mice ceased striving. The amount of time spent floating in the water and the slightest movement necessary to keep afloat were also recorded by a tracking system (ANY-maze, Japan). The exam

lasted six minutes.

2.4. Morphological observations

2.4.1. HE staining

The slices were dewaxed with xylene, followed by gradient ethanol de-benzene and then stained the nuclei with hematoxylin. Next, the nuclei were stained with 10 ml/L hydrochloric acid ethanol back to the water and 10 ml/L eosin aqueous solution. The slices were dehydrated again with gradient ethanol and sealant for microscopic examination after clearing and observed under the microscope for morphological changes in hippocampus pathology.

2.4.2. Nissl staining

The slices were dewaxed and stained with tarry violet staining solution for 10 min at 37 °C. After rinsing with distilled water, the slices were washed with 70% and 95% ethanol until the Nissl was purple. Next, the slices were dehydrated, translucent and sealed. Finally, the results of the Nissl body were observed under a microscope.

2.5. Chemical treatment and cell culture

PC12 cells were purchased from the American Type Culture Collection (ATCC), a rat adrenal pheochromocytoma cell line that had been frequently employed in neuroscience research due to its many similarities to human neurons (Wiatrak, 2020). The cells were cultured at 37 °C in a humidified environment containing 5% CO_2 and in Dulbecco's Modified Eagle's Condition/Nutrient F-12 Ham medium (Gibico, USA), supplemented with 10% (v/v) fetal bovine serum (Invitrogen, USA). The final NaF dose is determined by checking cell viability assessed by the Cell Counting Kit-8 with different NaF concentrations (10–80 mg/L). The logarithmic growth phase cells were divided into two groups: a control group and a test group that received 40 mg/L NaF (Zhou, 2021) for 24 h. For inhibiting test, cells were pre-treated with 10 μM Creb1 inhibitor 66615 for 2 h (Med Chem Express, USA) to reduce p-Creb1.

2.6. Western blotting results

Following treatment, the male offspring hippocampus tissue and PC12 cells were homogenized in RIPA buffer (Beyotime Institute of Biotechnology, China) for 30 min on ice before being centrifuged at 12,000 rpm and 4 °C for 30 min. A bicinchoninic acid (BCA) protein assay kit (Beyotime Institute of Biotechnology, China) was used to evaluate the protein level of the supernatant. Before being boiled for 5 min, the samples were diluted with loading buffer to achieve an equal concentration. Proteins were separated on a 7.5–15% SDS-PAGE gel, transferred to NC membranes (Pall, Inc., Mexico), and blocked for one hour at room temperature in Phosphate-buffered saline containing 0.1% Tween-20 solution (PBST). Creb1 (1:1500; Proteintech, Inc., China), p-Creb1 (1:1000; Abclonal, Inc., China), BDNF (1:1000; Abcam, Inc., UK), TrkB (1:5000; Abcam, Inc., UK), PSD95 (1:3000; Proteintech, Inc., China), SYN (1:20000; Proteintech, Inc., China), Tubulin (1:5000, Bimake, Inc., China). After three times washing with PBST, the membranes were incubated for one hour at room temperature with HRP-conjugated goat anti-rabbit IgG or goat anti-mouse IgG antibody. The signals were detected using ECL reagents (NCM, Inc., China) after PBST washing, and the bands were scanned using chemiluminescence imaging equipment (Tanon, Shanghai, China).

2.7. Immunofluorescence

In 24-well plates, PC12 cells were seeded onto sterile coverslips. The PC12 cells were administered 40 mg/L NaF for 24 h. The coverslips were rinsed three times in PBS before being fixed in 4% paraformaldehyde (PFA) for 30 min, then washed three times in PBS before being permeabilized with 0.1% Triton X-100 for 30 min. After 3 min of PBS washing, the coverslips were incubated with rhodamine phalloidin at room temperature for one hour while being kept away from light. Coverslips were dyed for 15 min at room temperature with DAPI staining solution, then washed with PBS in the dark to show the nuclei. The slides were examined using an inverted fluorescence microscope (Nikon, Japan).

2.8. Statistical analysis

All data were calculated as the mean±SD. GraphPad Prism 8 was used for the statistical analysis (GraphPad Software Inc., La Jolla, CA, USA). The thickness of Nissl bodies and dense postsynaptic material was counted using Image J software (NIH). N means the total number of maternal mice used for each group, while n means total offspring from a single mother used. The Student's *t*-test was used to look at the differences between the two groups. A two-way ANOVA was employed to assess the differences between groups, followed by Bonferroni *post hoc* testing. Statistical significance was defined as a P value of less than 0.05.

3. Results

3.1. The establishment and identification of prenatal NaF exposure model

From gestation day 1 (GD1) to GD20, the pregnant mice were provided with a normal diet and water with 100 mg/L NaF to generate a prenatal NaF exposure mouse model (Fig. 1A). During pregnancy, female mice exposed to NaF turned the lower incisors white from yellow (Fig. 1B) and had significantly higher fluoride ion concentrations in their urine (Fig. 1C). There were no significant changes in body weight, water consumption, food intake, urine volume, gestation duration, and litter size in pregnant mice (Fig. 1D-I).

3.2. The effect of prenatal NaF exposure on fetal weight and Creb1/BDNF/TrkB pathway in the fetal hippocampus

On day 20 of gestation, fetal brain weight, body weight and brain weight to body weight ratio were determined. Fetal brain weight (Fig. 2A) and body weight (Fig. 2B) were drastically decreased, while the ratio of fetal brain weight/body weight increased (Fig. 2C). To determine if the Creb1/BDNF/TrkB pathway in the fetal hippocampus was affected, we measured the levels of Creb1, p-Creb1, SYN and PSD95 in the NaF group compared to the control group. The NaF group had significantly elevated pro-BDNF levels and p-Creb1 and decreased TrkB levels (Fig. 2D). Our findings indicated that prenatal NaF exposure disrupts the p-Creb1-BDNF-TrkB signaling pathway during the early stages of development.

3.3. Prenatal NaF exposure induced learning and memory deficits in male offspring mice

There were no significant changes in body weight (Fig. 3A) and serum fluoride ion levels (Fig. 3B) in male offspring exposed to NaF from 1 to 6 weeks after birth. The escape latency of the NaF group was significantly higher than that of the control group for the whole training period of the location navigation test (Fig. 3C), while there was no significant difference in swimming speed between the two groups (Fig. 3D). A schematic representation of the positioning navigation test is shown in Fig. 3E. During the space trial test, the NaF group had much fewer crossing platforms and spent significantly less time in the target quadrant than the control group (Fig. 3F, G). A schematic representation of the space trial test is shown in Fig. 3H. These data showed prenatal NaF exposure reduces the cognitive performance of male offspring mice.

3.4. Prenatal NaF exposure did not affect emotional behavior

The rotarod test provides a convenient method for testing motor

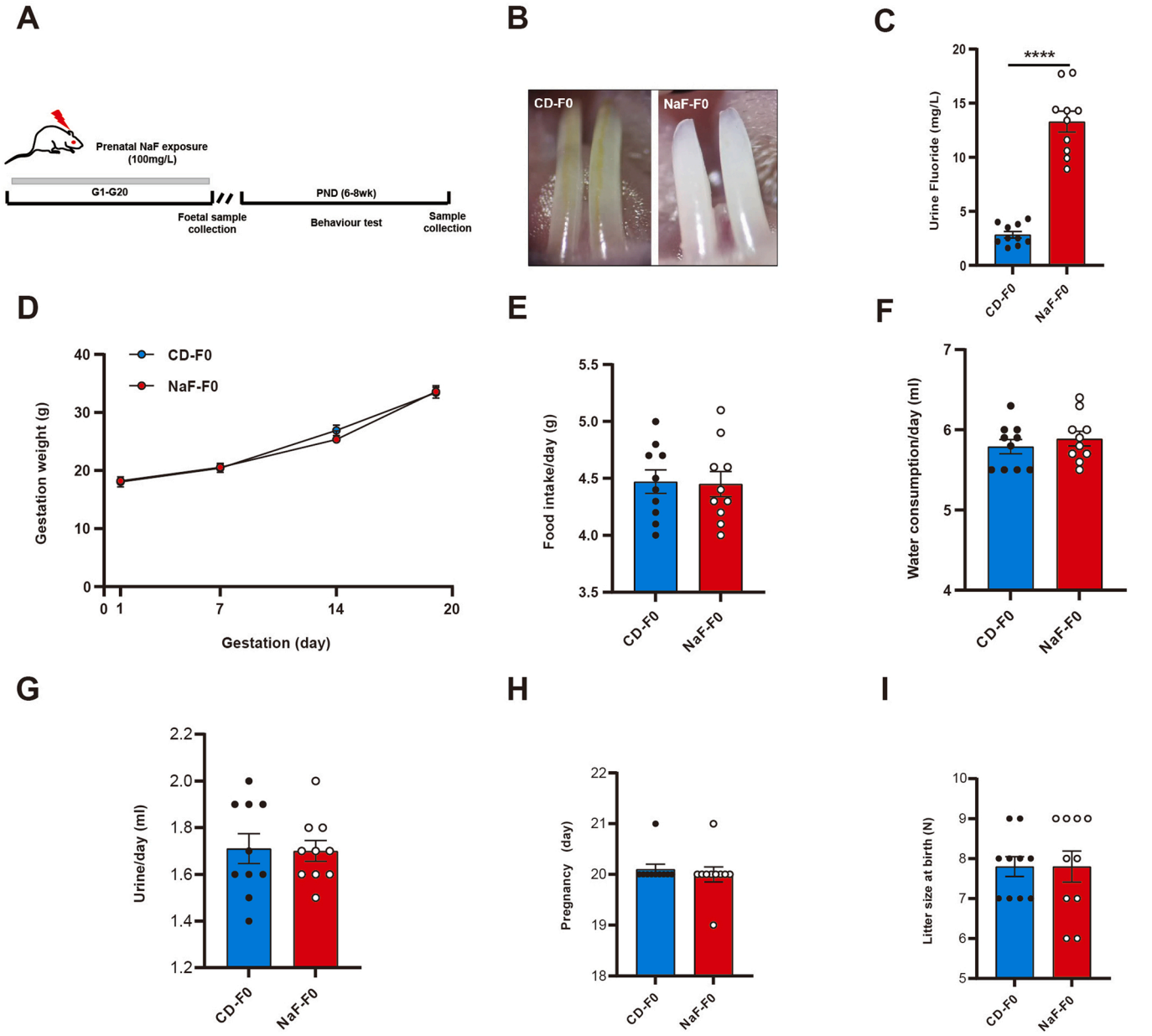

Fig. 1. The establishment and identification of the prenatal NaF exposure model. Schematic diagram of the experimental model (A). The tooth color of pregnant mice (B) and fluoride ion concentration in pregnant mice's urine (C) in two groups. The two groups' body weight (D), water intake (E), food consumption (F), urine volume (G), gestation time (H) and litter size (I). CD stands for the control, * $P < 0.05$, **** $P < 0.0001$, NaF group (N = 10) *vs.* the control group (N = 10). Values were calculated as mean ± SD.

function in rodents. Regardless of the stay rod time (Supplement 1A) or drop speed (Supplement 1B), there was no significant difference between the two groups, suggesting that no anomalies in their motility were seen. The open field test is the classical test paradigm that is generally accepted for measuring anxiety, exploratory behavior and locomotor behavior in animals. No significant differences were seen in the number of times entering the central area (Supplement 1C), the time in the central region and the time in the outside area (Supplement 1D). The elevated plus maze is an experimental approach for assessing rodent anxiety reactions. It has the benefit of being simple to conduct in comparison to mice's anxiety behaviors generated by damaging stimuli and it may visibly depict mice's conditioned reactions. The findings indicated that there were no significant changes in the amount of time spent in the open and closed arms between the two groups (Supplement 1E). The traditional approaches for detecting depression-like behavior in mice are the tail suspension test and the forced swim test. In the tail suspension test, the results indicated no change in immobility time between the two groups (Supplement 1F), as were the results of the forced swim test (Supplement 1G).

3.5. *Prenatal NaF exposure affected morphological changes in male offspring mice*

HE and Nissl staining were used to examine the impact of NaF exposure during pregnancy on the structure of the offspring's hippocampus. HE staining revealed no apparent structural alterations (Fig. 4A, B). Nissl bodies are basophilic substances within the cytoplasm. Staining Nissl body by Nissl staining can be used to visualize the cellular structure within the neuron and evaluate neuronal damage and loss. Image J software was used to count the Nissl bodies between the two groups. It showed a substantial reduction of Nissl bodies in the NaF group, which indicated that fluoride exposure during pregnancy could

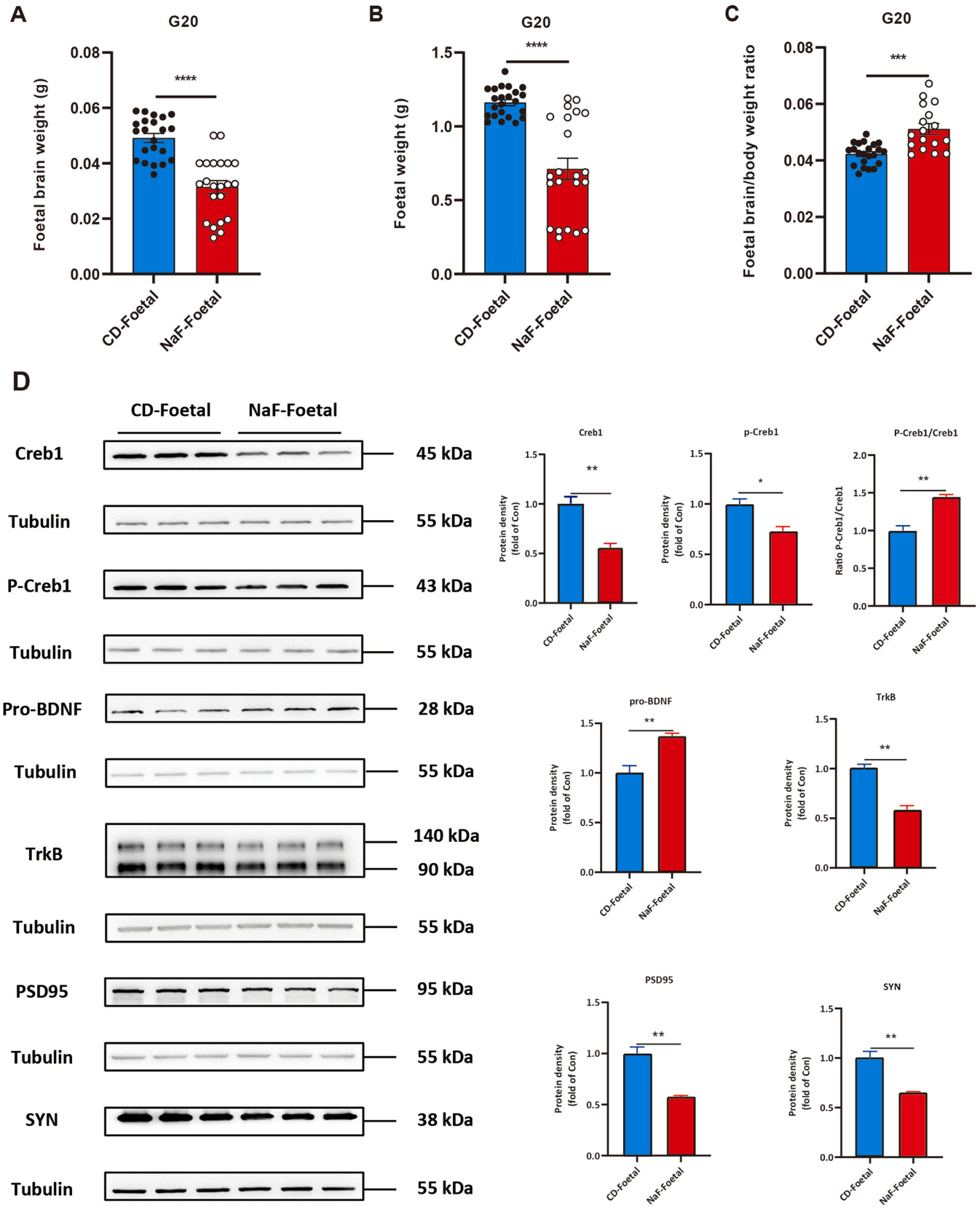

Fig. 2. The effect of prenatal NaF exposure on fetal weight and p-Creb1/BDNF/TrkB pathway in fetal. The fetal brain weight (A), body weight (B) and fetal brain weight/body weight ratio (C) (n = 22). Total Creb1, p-Creb1, pro-BDNF, TrkB, SYN and PSD95 protein abundance in the fetal hippocampus (D) (n = 6). CD stands for the control, * $P < 0.05$, ** $P < 0.01$, *** $P < 0.001$, **** $P < 0.0001$, the NaF group *vs.* the control group. Values were calculated as mean ± SD.

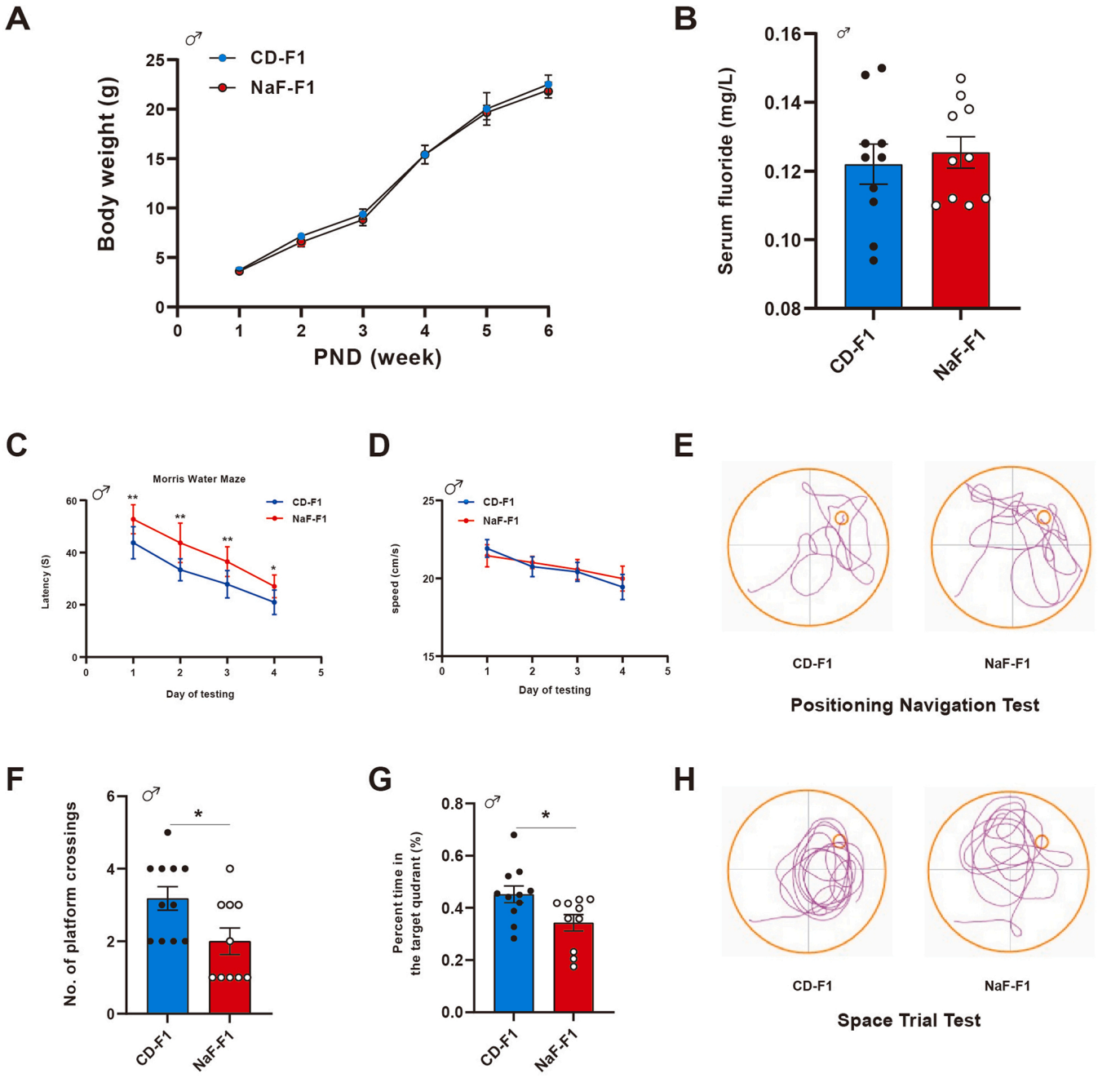

Fig. 3. Prenatal NaF exposure induced learning and memory deficits in male offspring mice. The two groups' body weight (A) (N = 10) and serum fluoride ion levels (B) (N = 10). The escape latency in the spatial position test (C). Mean swimming speed in the spatial position test (D). A schematic representation of the positioning navigation test (E). Crossing platforms in the target quadrant in the space trial test (F). The percent time in the target quadrant in the space trial test (G). A schematic representation of the space trial test (H). CD stands for the control, * $P < 0.05$, ** $P < 0.01$, the NaF group (n = 11) *vs.* the control group (n = 10). Values were calculated as mean ± SD.

lead to neuronal damage in male offspring (Fig. 4C-E).

3.6. Prenatal NaF exposure reduced dendritic spine density and synaptic protein expression linked to p-Creb1/BDNF/TrkB pathway disruption in male offspring mice

To determine if prenatal fluoride exposure induced cognitive deficits are linked to synaptic damage, we employed transmission electron microscopy to study alterations in the hippocampus's ultrastructure. The findings indicated that the NaF group had an altered synaptic ultrastructure in the hippocampus. The hippocampal neuron nuclei in the control group were round and large, while those in the NaF group showed atrophy and irregular shape (Fig. 5A). Mice in the NaF group had widened synaptic gaps and thinner postsynaptic density (Fig. 5B-D). Additionally, pre-and postsynaptic markers SYN and PSD95 were decreased in the NaF group. Meanwhile, total Creb1 protein levels remained unchanged, but p-Creb1 and pro-BDNF levels in the NaF group increased significantly, while TrkB levels decreased (Fig. 5E). Taken together, our findings implied that prenatal NaF exposure impaired hippocampus cell spinogenesis and synaptogenesis, as well as disrupted p-Creb1-BDNF-TrkB transmission in male offspring mice.

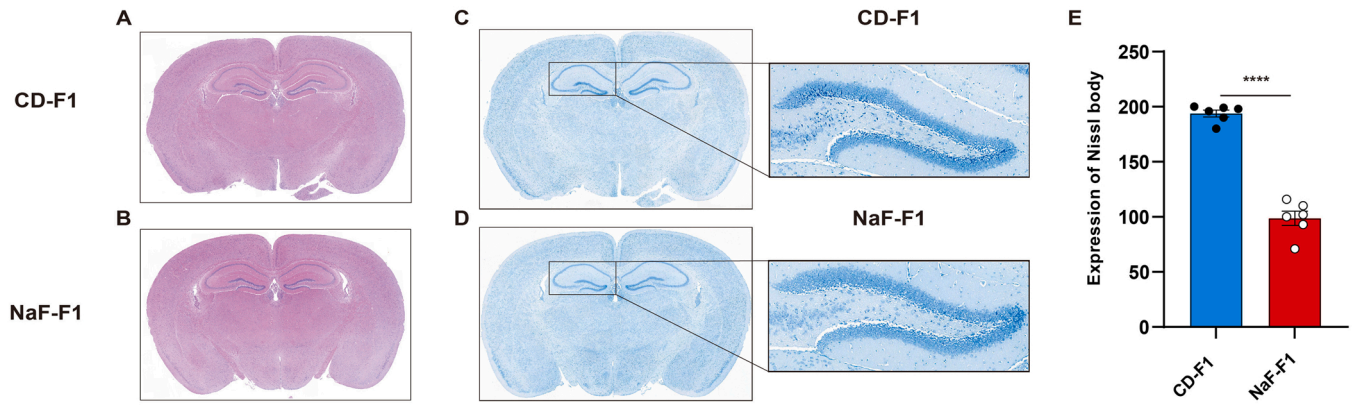

Fig. 4. Prenatal NaF exposure affected morphological changes in male offspring mice. HE staining (A, B) and Nissl staining (C, D). Expression of Nissl bodies (E). CD stands for the control, **** $P < 0.0001$, the NaF group (n = 3) *vs.* the control group (n = 3). Values were calculated as mean ± SD.

3.7. NaF-induced disruption of p-Creb1-BDNF-TrkB pathway and cytoskeleton abnormalities in PC12 cells

We used CCK8 to test the toxicity of various NaF concentrations on PC12 cells. After 24 h, different NaF concentrations were employed to treat PC12 cells, and a final concentration of 40 mg/L NaF was calculated for the following study (Fig. 6A). Simultaneously, by rhodamine phalloidin labeling, the impact of 40 mg/L NaF this concentration on the cytoskeleton was determined. The cytoskeleton of PC12 treated with NaF did not stain much, while the control group exhibited evident clustered myofilaments, indicating NaF affects F-actin aggregation (Fig. 6B).

The BDNF-TrkB axis was discovered due to the importance of BDNF-TrkB signaling in the formation and maintenance of synapses. As demonstrated in Fig. 6C, the 40 mg/L NaF group drastically lowered TrkB levels while increasing pro-BDNF levels considerably, indicating that BDNF-TrkB signaling was disrupted. Then, we evaluated if the aberrant alterations in BDNF-TrkB signaling are caused by p-Creb1. The 40 mg/L NaF group dramatically increased the level of p-Creb1 in comparison to the control group while decreasing SYN and PSD95 expression drastically. Intriguingly, 66615, an inhibitor of Creb1, restored the abnormal BDNF signaling, PSD95 and TrkB expression produced by NaF treatment. Our results suggested that p-Creb1 was influential in the development and maintenance of NaF-induced dysregulation through the BDNF-TrkB pathway.

4. Discussions

Endemic fluorosis, an endemic condition caused by prolonged fluoride exposure, was recognized as a severe public health hazard in many developing nations where significant fluorine contamination of drinking water had been seen (Grandjean, 2019). According to reports, China and India are the most impacted countries, with fluorine concentrations in groundwater reaching 48 mg/L (Feng et al., 2020; Mridha et al., 2021). Endemic fluorosis is present in at least 20 states of India, affecting more than 65 million people, including 6 million children. Fluoride ion (F) concentrations in India's groundwater vary widely, ranging from 0.01 mg/L to 48 mg/L. (Chakrabarty, 2012) In Datong Basin, Shanxi Province, China, groundwater fluoride ion concentrations are up to 22 mg/L (about 48 mg/L sodium fluoride). (Wen, 2013) Based on previous research, Chen et al. successfully established a rat model by selecting fluoride concentrations (as 10, 50, and 100 mg/L NaF, respectively, corresponding to 4.52, 22.6, and 45.2 mg/L fluorine ion) that took into account both the real-world human exposure situation (concentration, mode, and duration) and rats' superior ability to clear fluoride from their bodies (Chen et al., 2018). Therefore, 100 mg/L NaF was used in our study to establish a prenatal fluoride exposed mouse model. In our NaF model, the ratio of fetal brain weight to body weight was increased, indicating an increase in relative fetal brain weight in the NaF group. It might be due to an intrinsic mechanism protecting vital organs from threatening risks such as NaF. However, although this ratio suggested a possible protective mechanism, fetal brain development was still affected by prenatal NaF exposure, as evidenced by brain weight loss compared to the control group.

Our findings showed that prenatal fluoride exposure impaired cognitive abilities in male offspring mice, which backs up previous findings that excessive fluoride exposure caused behavioral abnormalities in humans and rodents, including inattention, memory and cognitive performance deficits, implying that the present mouse model of prenatal fluoride exposure is well established. In addition, the rotarod fatigue test, open field test, elevated plus maze test, tail suspension test and forced swimming test were conducted to see if NaF exposure during pregnancy affected offspring motor abilities, anxiety and depression-like behaviors. According to the results, there was no significant difference between the NaF and control groups. Our findings suggested that prenatal NaF exposure affected learning and memory abilities other than emotional behaviors.

The current research investigated alterations of the synaptic morphology and relative proteins in the hippocampus to learn more about the developmental neurotoxicity caused by prenatal fluoride exposure. Scanning using a transmission electron microscope (TEM) is a traditional way of obtaining comprehensive information on the morphological properties of neurons. By TEM, mice in the NaF group were found to have impaired hippocampus synaptic ultrastructure, widened synaptic gaps and thinner postsynaptic density. In NaF-treated PC12 cells, morphological alterations in the cytoskeleton were identified, corroborating ours *in vivo* findings. These findings suggested that embryonic fluoride exposure produces morphological changes in dendrites and synapses, which are closely linked to cognitive impairment. Prenatal fluoride exposure also decreased the protein abundance of the postsynaptic marker PSD95 and the presynaptic protein SYN *in vivo* and *in vitro*. PSD95 is the PSD's most abundant protein and is involved in neurotransmission, synaptic plasticity and dendritic spine formation during neurodevelopment. PSD95 had been found to traffic growth-promoting PSD proteins out of the active spine during plasticity induction, triggering and then terminating spine development (Steiner et al., 2008). Accordingly, fluoride-induced downregulation of PSD95 protein expression in synapses might result in PSD protein transportation failure, disrupt the creation and maintenance of the spine, then cause impairment. SYN is a presynaptic marker whose expression accurately reflects the quantity and density of synapses and the state of synaptogenesis (Lepeta et al., 2016). In our mouse model, a decrease in synaptic membrane fluidity and decreased levels of PSD95 and SYN were found in the male offspring hippocampus, indicating that high NaF exposure

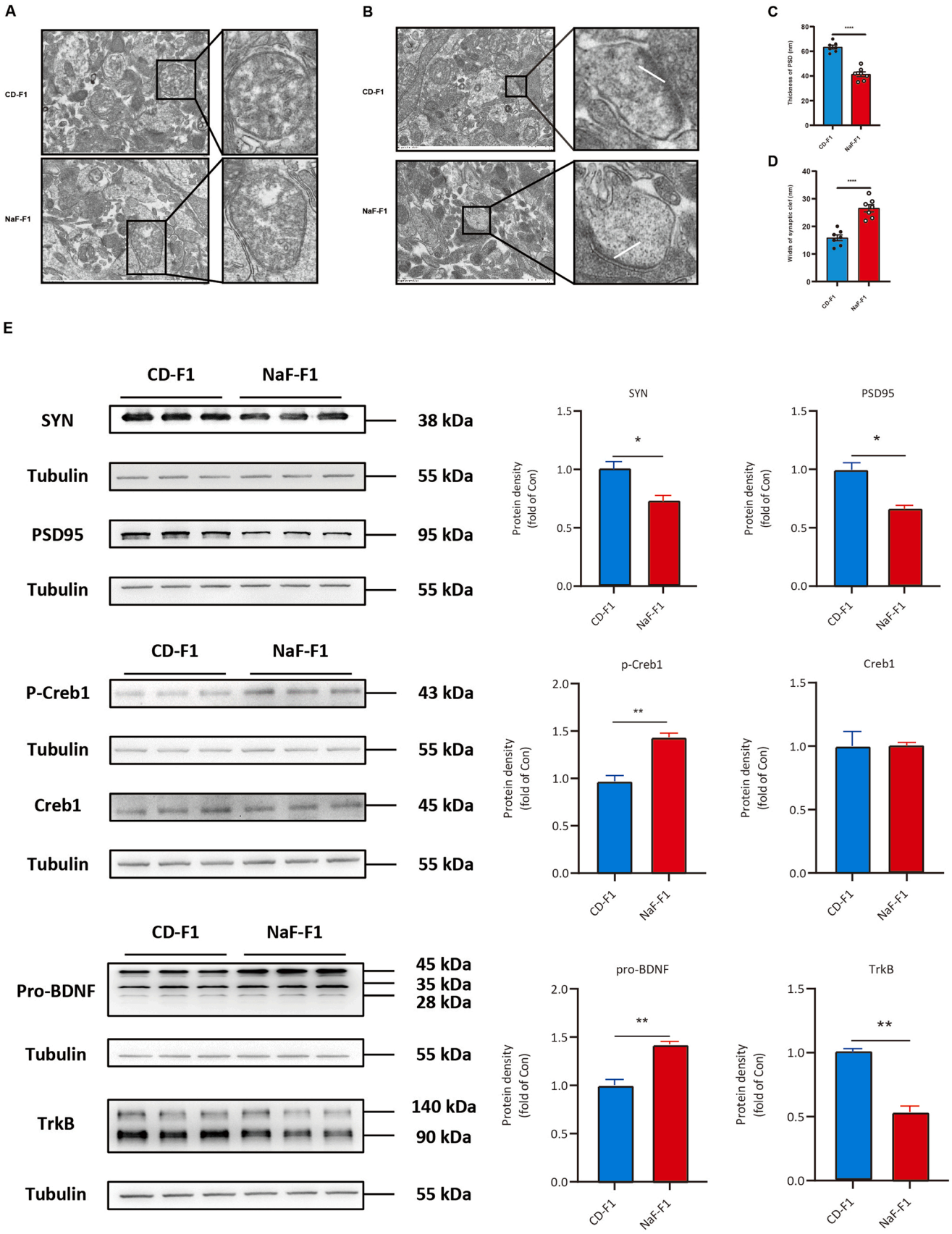

Fig. 5. Prenatal NaF exposure reduced dendritic spine density and synaptic protein expression linked to p-Creb1/BDNF/TrkB signaling disruption in male offspring mice. The hippocampus neuron nuclei (A), synaptic clefts and postsynaptic densities (B) (n = 3). Synaptic clefts and postsynaptic densities in two groups (C, D). Total Creb1, p-Creb1, pro-BDNF, TrkB, SYN and PSD95 protein abundance in two groups (E) (n = 6). CD stands for the control, * $P < 0.05$, ** $P < 0.01$, **** $P < 0.0001$, the NaF group *vs.* the control group. Values were calculated as mean ± SD.

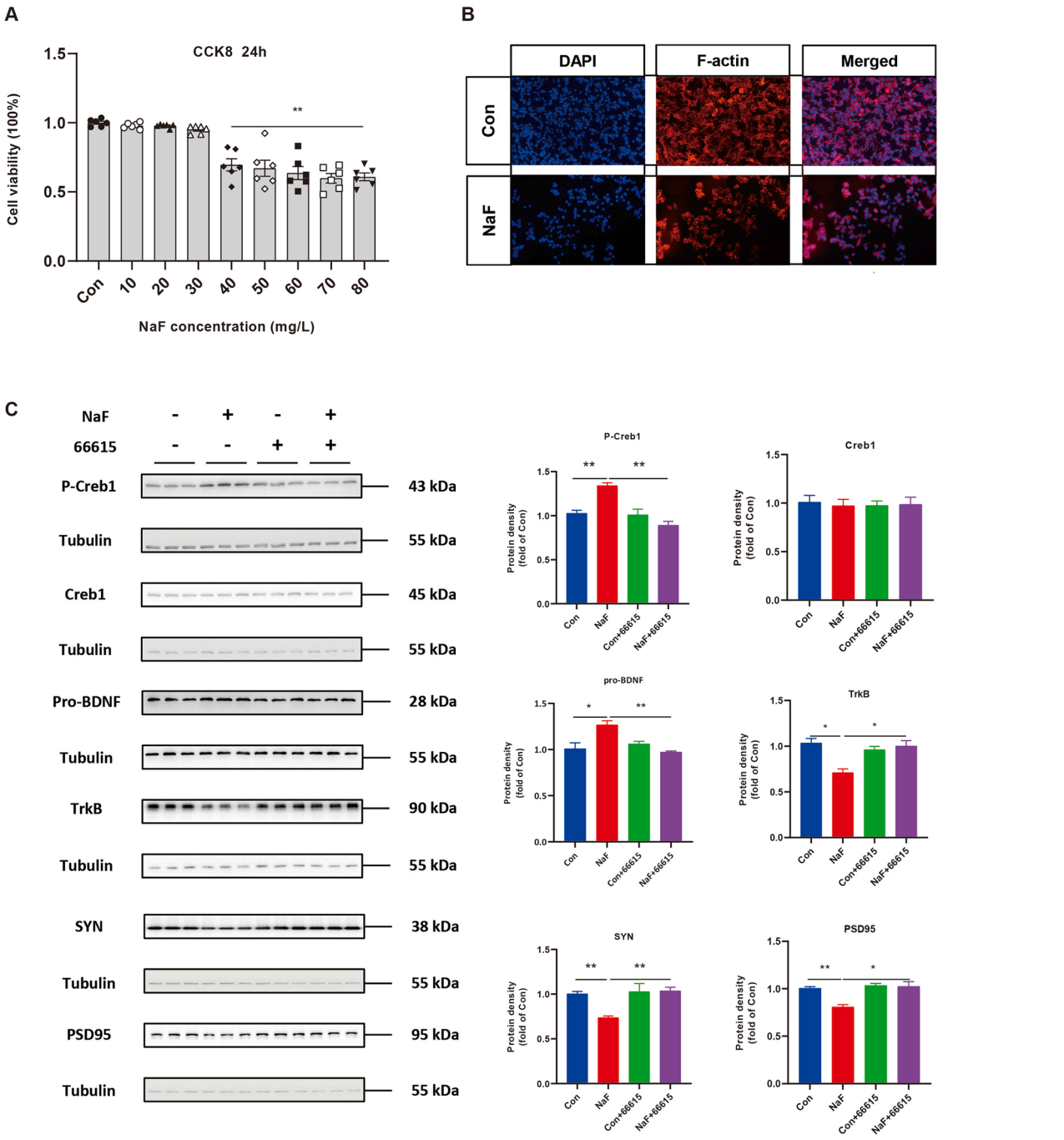

Fig. 6. NaF-induced disruption of the p-Creb1-BDNF-TrkB pathway and cytoskeleton abnormalities in PC12 cells. The CCK8 test (A) (n = 3). The cytoskeleton staining with rhodamine phalloidin labeling (B) (n = 3). Total Creb1, p-Creb1, pro-BDNF, TrkB, SYN and PSD95 protein abundance (C) (n = 3). * $P < 0.05$, ** $P < 0.01$ *vs.* the control group. Values were calculated as mean ± SD.

impaired spinogenesis and synaptogenesis in neurons.

During the development and maturation phases of the brain, BDNF promotes dendritic and axonal growth, as well as synaptogenesis (Miranda et al., 2019). Surprisingly, higher BDNF levels in the NaF group were found both *in vivo* and *in vitro*, which is consistent with the findings of Chen et al. (Chen et al., 2018). We suspected this is due to a rise of BDNF precursors, also known as pro-BDNF, which have an opposite effect as the mature body. Accumulation of the pro-BDNF will lead to deleterious impacts eventually (Kowianski et al., 2018). Furthermore, accumulated evidence has shown that BDNF is significantly increased in neurons in response to different chemical stimulations, both *in vivo* and *in vitro* (Jiang et al., 2014; Chen et al., 2018; Zhou et al., 2021). In places with high lead content, children's blood BDNF levels rose and their olfactory memory decreased (Zhang et al., 2017). Furthermore, TrkB (BDNF receptor) plays essential functions in dendritic expansion and synapse formation. As a result, we discovered a significant decrease in TrkB levels in both *in vivo* and *in vitro* fluoride exposure models. These findings indicated that prenatal fluoride exposure induced neurotoxicity is associated with a disruption in the BDNF-TrkB pathway.

Creb1 is crucial in the development and function of the brain. Developmental disorders, such as poor cognitive function, may be caused by mutations or deletions of components in the Creb1 signaling cascade (Sakamoto et al., 2011). Phosphorylated Creb1 promotes

dendritic spine formation in most cases (Murphy and Segal, 1997). However, the present finding revealed the increased p-Creb1 level in the NaF mice hippocampus and NaF-treated PC12 cells. To learn more about how the involvement of Creb1 in prenatal fluoride exposure caused synaptogenesis impairment, we pre-treated NaF-exposed PC12 cells with 66615, the inhibitor of Creb1, which could inhibit Creb1 phosphorylation effectively (Zhang et al., 2019). Interestingly, inhibition of p-Creb1 restored the levels of PSD95, SYN, TrkB and BDNF proteins. Creb1, a classical transcriptional regulator, can bind to BDNF and affect BDNF expression (Esvald et al., 2020). As we know that TrkB can be regulated by BDNF since it is a BDNF receptor. However, the regulation of TrkB may also be independent of its ligand. Serra et al. reported that BCP administration had an opposite effect on BDNF and TrkB. It showed that the decrement of BDNF along with an increment of TrkB (Serra et al., 2022). They explained this BDNF-TrkB mismatch by the interaction of the TrkB with products of the complex molecular network induced by BCP. Therefore, in our study, the administration of 66615 may also induce the production of some molecules similar to CB1, and lead to the increase of TrkB. 66615 could reduce seizure severity in the intra-amygdala kainic acid model (Conte et al., 2020). Behavioral assays also showed significantly attenuated aggression in 66615-treated social isolation male mice (Wang et al., 2022). Also, peripheral non-specific inhibition of Creb1 by 66615 reversed pain sensitivity and anxiodepression induced by peripheral nerve injury (Wen et al., 2022). To a certain extent, the above studies may suggest that 66615 has a "neuroprotective effect". In our study, we found that exposure to fluoride induced neurotoxicity and reduced TrkB expression both *in vivo* and *in vitro*. Therefore, 66615 could rescue TrkB expression through its neuroprotective function rather than the BDNF-TrkB signaling pathway to alleviate the neurotoxicity of sodium fluoride. These findings showed that p-Creb1 interferes with BDNF-TrkB signaling, resulting in prenatal fluoride exposure induced synaptogenesis dysfunction.

5. Conclusions

In this work, we employed *in vivo* and *in vitro* data to demonstrate that prenatal fluoride exposure triggered neurotoxicity is connected to synaptogenesis malfunction. We discovered that fluoride exposure increased p-Creb1 induces BDNF-TrkB signaling disruption, which results in deficient synaptogenesis. Inhibition of p-Creb1 may be a viable therapeutic target to minimize synaptic failure in the presence of fluoride. These results allowed us to understand the routes of fluoride-induced developmental neurotoxicity better.

CRediT authorship contribution statement

Weisheng Li, Likui Li, Dan Zhu, Jingliu Liu, Yajun Shi: Conceptualization. **Hongtao Zeng, Xi Yu, Jun Guo, Bin Wei, Yongle Cai**: Data curation. **Hongtao Zeng, Xi Yu, Jun Guo, Bin Wei, Yongle Cai**: Formal analysis. **Miao Sun**: Funding acquisition, Supervision. **Weisheng Li, Likui Li**: Methodology. **Weisheng Li, Likui Li**: Writing – original draft. **Weisheng Li, Likui Li, Dan Zhu, Jingliu Liu, Miao Sun**: Writing – reiew &editing.

Funding

This work was supported by grants from the National Key R&D Program of China (2019YFA0802600), and the National Natural Science Foundation of China (81974244 and 81570960).

Conflict of interest statement

The authors declared that there are no potential conflicts of interest.

Declaration of Competing Interest

The authors declare that they have no known competing financial interests or personal relationships that could have appeared to influence the work reported in this paper.

Appendix A. Supporting information

Supplementary data associated with this article can be found in the online version at doi:10.1016/j.ecoenv.2022.113682.

References

Adkins, E.A., Brunst, K.J., 2021. Impacts of fluoride neurotoxicity and mitochondrial dysfunction on cognition and mental health: a literature review. Int. J. Environ. Res. Public Health 18 (24), 12884. https://doi.org/10.3390/ijerph182412884.

Blaylock, R.L., 2004. Excitotoxicity: A possible central mechanism in fluoride neurotoxicity. Fluoride 37 (4), 301–314.

Chen, J., Niu, Q., Xia, T., Zhou, G., Li, P., Zhao, Q., et al., 2018. ERK1/2-mediated disruption of BDNF-TrkB signaling causes synaptic impairment contributing to fluoride-induced developmental neurotoxicity. Toxicology 410, 222–230. https://doi.org/10.1016/j.tox.2018.08.009.

Conte, G., Parras, A., Alves, M., Olla, I., De Diego-Garcia, L., Beamer, E., et al., 2020. High concordance between hippocampal transcriptome of the mouse intra-amygdala kainic acid model and human temporal lobe epilepsy. Epilepsia 61 (12), 2795–2810. https://doi.org/10.1111/epi.16714.

Darchen, A., Sivasankar, V., Prabhakaran, M., et al., 2016. Health effects of direct or indirect fluoride ingestion[M]//Surface Modified Carbons as Scavengers for Fluoride from Water. Springer, Cham, pp. 33–62. https://doi.org/10.1007/978-3-319-40686-2_3.

Esvald, E.E., Tuvikene, J., Sirp, A., Patil, S., Bramham, C.R., Timmusk, T., 2020. CREB Family Transcription Factors Are Major Mediators of BDNF Transcriptional Autoregulation in Cortical Neurons. J. Neurosci. 40 (7), 1405–1426. https://doi.org/10.1523/JNEUROSCI.0367-19.2019.

Feng, F., Jia, Y., Yang, Y., Huan, H., Lian, X., Xu, X., et al., 2020. Hydrogeochemical and statistical analysis of high fluoride groundwater in northern China. Environ. Sci. Pollut. Res. Int. 27 (28), 34840–34861. https://doi.org/10.1007/s11356-020-09784-z.

Flace, P., Benagiano, V., Vermesan, D., Sabatini, R., Inchingolo, A.M., Auteri, P., et al., 2010. Effects of developmental fluoride exposure on rat ultrasonic vocalization, acoustic startle reflex and pre-pulse inhibition. Eur. Rev. Med. Pharmacol. Sci. 14 (6), 507–512.

Grandjean, P., 2019. Developmental fluoride neurotoxicity: an updated review. Environ. Health 18 (1), 110. https://doi.org/10.1186/s12940-019-0551-x.

Green, R., Lanphear, B., Hornung, R., Flora, D., Martinez-Mier, E.A., Neufeld, R., et al., 2019. Association between maternal fluoride exposure during pregnancy and IQ scores in offspring in Canada. Jama Pediatrics 173 (10), 940–948. https://doi.org/10.1001/jamapediatrics.2019.1729.

Guth, S., Huser, S., Roth, A., Degen, G., Diel, P., Edlund, K., et al., 2020. Toxicity of fluoride: critical evaluation of evidence for human developmental neurotoxicity in epidemiological studies, animal experiments and in vitro analyses. Arch. Toxicol. 94 (5), 1375–1415. https://doi.org/10.1007/s00204-020-02725-2.

Jiang, C., Zhang, S., Liu, H., Guan, Z., Zeng, Q., Zhang, C., et al., 2014. Low glucose utilization and neurodegenerative changes caused by sodium fluoride exposure in rat's developmental brain. Neuromolecular Med. 16 (1), 94–105. https://doi.org/10.1007/s12017-013-8260-z.

Kowianski, P., Lietzau, G., Czuba, E., Waskow, M., Steliga, A., Morys, J., 2018. BDNF: a key factor with multipotent impact on brain signaling and synaptic plasticity. Cell Mol. Neurobiol. 38 (3), 579–593. https://doi.org/10.1007/s10571-017-0510-4.

Kraeuter, A.K., Guest, P.C., Sarnyai, Z., 2019. The elevated plus maze test for measuring anxiety-like behavior in rodents. Methods Mol. Biol. 1916, 69–74. https://doi.org/10.1007/978-1-4939-8994-2_4.

Lepeta, K., Lourenco, M.V., Schweitzer, B.C., Martino Adami, P.V., Banerjee, P., Catuara-Solarz, S., et al., 2016. Synaptopathies: synaptic dysfunction in neurological disorders - A review from students to students. J. Neurochem. 138 (6), 785–805. https://doi.org/10.1111/jnc.13713.

Li, C., Yan, Y., Cheng, J., Xiao, G., Gu, J., Zhang, L., et al., 2016. Toll-like receptor 4 deficiency causes reduced exploratory behavior in mice under approach-avoidance conflict. Neurosci. Bull. 32 (2), 127–136. https://doi.org/10.1007/s12264-016-0015-z.

Miranda, M., Morici, J.F., Zanoni, M.B., Bekinschtein, P., 2019. Brain-derived neurotrophic factor: a key molecule for memory in the healthy and the pathological brain. Front. Cell Neurosci. 13, 363. https://doi.org/10.3389/fncel.2019.00363.

Mridha, D., Priyadarshni, P., Bhaskar, K., Gaurav, A., De, A., Das, A., et al., 2021. Fluoride exposure and its potential health risk assessment in drinking water and staple food in the population from fluoride endemic regions of Bihar, India. Groundwater Sustain. Dev. 13, 100558.

Murphy, D.D., Segal, M., 1997. Morphological plasticity of dendritic spines in central neurons is mediated by activation of cAMP response element binding protein. Proc, Natl. Acad. Sci. U. S. A. 94 (4), 1482–1487. https://doi.org/10.1073/pnas.94.4.1482.

Qiu, L.L., Pan, W., Luo, D., Zhang, G.F., Zhou, Z.Q., Sun, X.Y., et al., 2020. Dysregulation of BDNF/TrkB signaling mediated by NMDAR/Ca(2+)/calpain might contribute to postoperative cognitive dysfunction in aging mice. J. Neuroinflammation. 17 (1), 23. https://doi.org/10.1186/s12974-019-1695-x.

Rasool, A., Farooqi, A., Xiao, T., Ali, W., Noor, S., Abiola, O., et al., 2018. A review of global outlook on fluoride contamination in groundwater with prominence on the Pakistan current situation. Environ. Geochem Health 40 (4), 1265–1281. https://doi.org/10.1007/s10653-017-0054-z.

Sakamoto, K., Karelina, K., Obrietan, K., 2011. CREB: a multifaceted regulator of neuronal plasticity and protection. J. Neurochem. 116 (1), 1–9. https://doi.org/10.1111/j.1471-4159.2010.07080.x.

Serra, M.P., Boi, M., Carta, A., Murru, E., Carta, G., Banni, S., et al., 2022. Anti-Inflammatory Effect of Beta-Caryophyllene Mediated by the Involvement of TRPV1, BDNF and trkB in the Rat Cerebral Cortex after Hypoperfusion/Reperfusion. Int. J. Mol. Sci. 23 (7) https://doi.org/10.3390/ijms23073633.

Steiner, P., Higley, M.J., Xu, W., Czervionke, B.L., Malenka, R.C., Sabatini, B.L., 2008. Destabilization of the postsynaptic density by PSD-95 serine 73 phosphorylation inhibits spine growth and synaptic plasticity. Neuron 60 (5), 788–802. https://doi.org/10.1016/j.neuron.2008.10.014.

Strunecka, A., Strunecky, O., 2019. Chronic fluoride exposure and the risk of autism spectrum disorder. Int. J. Environ. Res. Public Health 16 (18), 3431. https://doi.org/10.3390/ijerph16183431.

Wang, Z.J., Shwani, T., Liu, J., Zhong, P., Yang, F., Schatz, K., et al., 2022. Molecular and cellular mechanisms for differential effects of chronic social isolation stress in males and females. Mol. Psychiatry 1–13. https://doi.org/10.1038/s41380-022-01574-y.

Wen, J., Xu, Y., Yu, Z., Zhou, Y., Wang, W., Yang, J., et al., 2022. The cAMP Response Element- Binding Protein/Brain-Derived Neurotrophic Factor Pathway in Anterior Cingulate Cortex Regulates Neuropathic Pain and Anxiodepression Like Behaviors in Rats. Front. Mol. Neurosci. 15, 831151 https://doi.org/10.3389/fnmol.2022.831151.

Wu, Y., Wang, M., Wang, Y., Yang, H., Qi, H., Seicol, B.J., et al., 2020. A neuronal wiring platform through microridges for rationally engineered neural circuits. APL Bioeng. 4 (4), 046106 https://doi.org/10.1063/5.0025921.

Yoshii, A., Constantine-Paton, M., 2010. Postsynaptic BDNF-TrkB signaling in synapse maturation, plasticity, and disease. Dev. Neurobiol. 70 (5), 304–322. https://doi.org/10.1002/dneu.20765.

Zhang, B., Huo, X., Xu, L., Cheng, Z., Cong, X., Lu, X., et al., 2017. Elevated lead levels from e-waste exposure are linked to decreased olfactory memory in children. Environ. Pollut. 231 (Pt1), 1112–1121. https://doi.org/10.1016/j.envpol.2017.07.015.

Zhang, B., Zhang, P., Tan, Y., Feng, P., Zhang, Z., Liang, H., et al., 2019. C1q-TNF-related protein-3 attenuates pressure overload-induced cardiac hypertrophy by suppressing the p38/CREB pathway and p38-induced ER stress. Cell Death Dis. 10 (7), 520. https://doi.org/10.1038/s41419-019-1749-0.

Further reading

Cao, J., Chen, Y., Chen, J., Yan, H., Li, M., Wang, J., 2016. Fluoride exposure changed the structure and the expressions of Y chromosome related genes in testes of mice. Chemosphere 161, 292–299. https://doi.org/10.1016/j.chemosphere.2016.06.106.

Chakrabarty, S., Sarma, H., 2012. Defluoridation of contaminated drinking water using neem charcoal adsorbent: kinetics and equilibrium studies. Int. J. ChemTech Res. 4 (2), 511–516.

DenBesten, P., Li, W., 2011. Chronic fluoride toxicity: dental fluorosis. Monogr. Oral. Sci. 22, 81–96. https://doi.org/10.1159/000327028.

Fu, R., Niu, R., Zhao, F., Wang, J., Cao, Q., Yu, Y., et al., 2022. Exercise alleviated intestinal damage and microbial disturbances in mice exposed to fluoride. Chemosphere 288 (Pt 3), 132658. https://doi.org/10.1016/j.chemosphere.2021.132658.

Lyaruu, D.M., Bronckers, A.L., Santos, F., Mathias, R., DenBesten, P., 2008. The effect of fluoride on enamel and dentin formation in the uremic rat incisor. Pediatr. Nephrol. 23 (11), 1973–1979. https://doi.org/10.1007/s00467-008-0890-2.

Wang, D.M., Cao, L.Y., Pan, S.J., Wang, G., Wang, L.W., Cao, N.Y., et al., 2021. Sirt3-mediated mitochondrial dysfunction is involved in fluoride-induced cognitive deficits. Food Chem. Toxicol. 158, 112665 https://doi.org/10.1016/j.fct.2021.112665.

Wen, D.G., Zhang, F.C., Zhang, E.Y., Wang, C., Han, S.B., Zheng, Y., 2013. Arsenic, fluoride and iodine in groundwater of China. J. Geochem. Explor. 135, 1–21. https://doi.org/10.1016/j.gexplo.2013.10.012.

Wiatrak, B., Kubis-Kubiak, A., Piwowar, A., Barg, E., 2020. PC12 cell line: cell types, coating of culture vessels, differentiation and other culture conditions. Cells 9 (4), 958. https://doi.org/10.3390/cells9040958.

Zhou, G., Hu, Y., Wang, A., Guo, M., Du, Y., Gong, Y., et al., 2021. Fluoride stimulates anxiety- and depression-like behaviors associated with SIK2-CRTC1 signaling dysfunction. J. Agric Food Chem. 69 (45), 13618–13627. https://doi.org/10.1021/acs.jafc.1c04907.

Zhou, L., Tao, X., Pang, G., Mu, M., Sun, Q., Liu, F., et al., 2021. Maternal nicotine exposure alters hippocampal microglia polarization and promotes anti-inflammatory signaling in juvenile offspring in mice. Front. Pharmacol. 12, 661304 https://doi.org/10.3389/fphar.2021.661304.